Earth and Planetary Science Letters 496 (2018) 206–214

Contents lists available at ScienceDirect

Earth and Planetary Science Letters

www.elsevier.com/locate/epsl

Mars obliquity history constrained by elliptic crater orientations

Samuel J. Holo [a,*], Edwin S. Kite [a], Stuart J. Robbins [b]

[a] University of Chicago, Department of Geophysical Sciences, Chicago, IL 60637, United States
[b] Southwest Research Institute, Boulder, CO 80302, United States

ARTICLE INFO

Article history:
Received 11 September 2017
Received in revised form 24 May 2018
Accepted 26 May 2018
Available online xxxx
Editor: W.B. McKinnon

Keywords:
Mars
obliquity history
elliptic craters

ABSTRACT

The dynamics of Mars' obliquity are believed to be chaotic, and the historical ∼3.5 Gyr (late-Hesperian onward) obliquity probability density function (PDF) is highly uncertain and cannot be inferred from direct simulation alone. Obliquity is also a strong control on post-Noachian Martian climate, enhancing the potential for equatorial ice/snow melting and runoff at high obliquities ($\gtrsim 40°$) and enhancing the potential for desiccation of deep aquifers at low obliquities ($\lesssim 25°$). We developed a new technique using the orientations of elliptical craters to constrain the true late-Hesperian-onward obliquity PDF. To do so, we developed a forward model of the effect of obliquity on elliptic crater orientations using ensembles of simulated Mars impactors and ∼3.5 Gyr-long Mars obliquity simulations. In our model, the inclinations and speeds of Mars crossing objects bias the preferred orientation of elliptic craters which are formed by low-angle impacts. Comparison of our simulation predictions with a validated database of elliptic crater orientations allowed us to invert for the best-fitting obliquity history. We found that since the onset of the late Hesperian, Mars' mean obliquity was likely low, between ∼10° and ∼30°, and the fraction of time spent at high obliquities >40° was likely <20%.

1. Introduction

Mars' obliquity, ϵ, is currently ∼25° but has changed dramatically over billions of years since solar system formation (Ward, 1973; Touma and Wisdom, 1993; Laskar and Robutel, 1993; Laskar et al., 2004). The dynamics of Mars' obliquity are driven by secular spin-orbit resonances (Touma and Wisdom, 1993; Laskar and Robutel, 1993). However, the obliquity evolution is sensitive to orbital properties that vary chaotically on timescales <100 Myr (Touma and Wisdom, 1993; Laskar and Robutel, 1993; Laskar et al., 2004). Many geologic methods have been proposed to vault the fundamental barrier of the chaotic diffusion of the Solar System (e.g. Ma et al., 2017; Kent et al., 2018), but all are indirect. Further, no more than a few transitions between low and high values of ϵ should occur (Section 3.1), preventing variations in obliquity from "averaging out" over billions of years. Thus, both the full obliquity history and the historical obliquity probability density function (PDF) are highly uncertain. Here we propose a direct method to constrain obliquity history.

Obliquity variations are a strong control on post-Noachian Martian climate (Jakosky and Carr, 1985; Laskar et al., 2004). At low obliquities ($\lesssim 25°$), the Martian atmosphere is more likely to collapse at the poles (Kreslavsky and Head, 2005; Phillips et al., 2011; Soto et al., 2015) and surface melting is unlikely (Fastook et al., 2012). At high obliquities ($\gtrsim 40°$), models predict that water vapor pressure increases (Zent, 2013; Forget et al., 2017), surface melting is more likely (Jakosky and Carr, 1985), and strong dust storms initiate near the poles (Haberle et al., 2003). Insolation driven ice and snow melt has been proposed to explain observed sedimentary features near the equator (e.g. Kite et al., 2013; Irwin et al., 2015; Palucis et al., 2014). Further, low values of obliquity have been shown in models to dramatically enhance desiccation of deep aquifers via sublimation (Grimm et al., 2017).

To constrain the true effects of Mars' obliquity on post-Noachian climate, it is necessary to constrain the true obliquity history, and thus we sought a geologic constraint on Mars' obliquity history. Previous attempts to constrain Mars' obliquity from geologic features such as mid-latitude glaciers (e.g. Fassett et al., 2014) show that Mars' obliquity was high (∼35°) for ∼1 Gyr. However, no study has quantitatively constrained the full ∼3.5 Gyr post-Noachian Mars obliquity PDF with geologic evidence. Here, we propose a new method of constraining the historical Mars obliquity PDF using the orientations of elliptic craters. The vast majority of craters on Mars are nearly circular, but impactors with small impact angles relative to the surface produce elliptic craters with major axes aligned with impactor velocity vector

---

[*] Corresponding author.
E-mail address: holo@uchicago.edu (S.J. Holo).

https://doi.org/10.1016/j.epsl.2018.05.046
0012-821X/

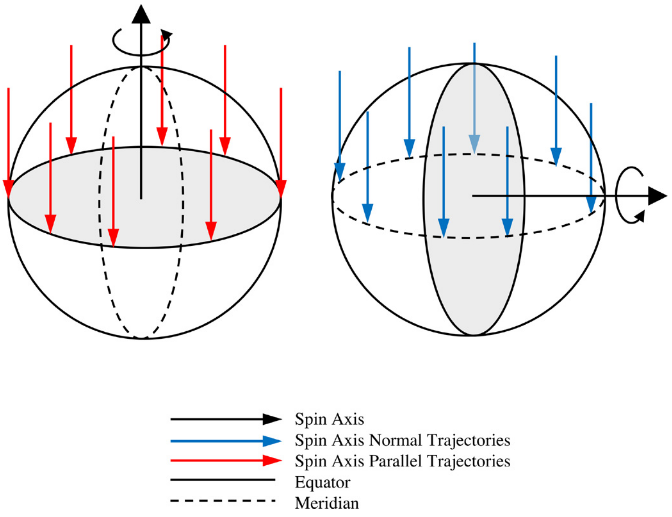

Fig. 1. Schematic illustrating the basic principle in our model. Spin axis parallel impactors create N–S elliptic craters near the equator, while spin axis normal impactors produce elliptic craters that are E–W oriented at all latitudes except near the pole. The effects of gravity focusing are not shown here for simplicity.

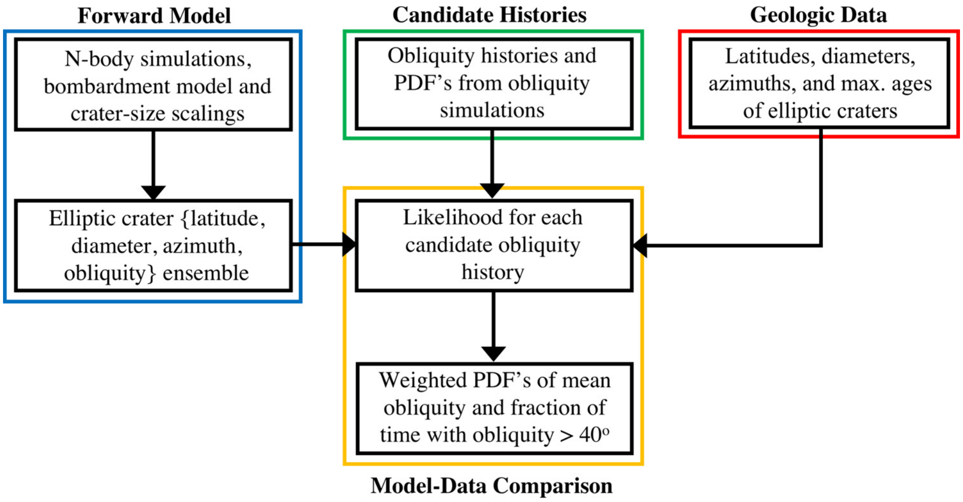

Fig. 2. Schematic showing our workflow.

(Bottke et al., 2000; Collins et al., 2011). As a result, impactors that travel parallel to Mars' spin pole will create North–South oriented craters at the equator, and impactors that travel normal to the spin pole will create elliptic craters at all latitudes that are East–West oriented everywhere except near the pole (Fig. 1). As the obliquity changes, the angles between impactors and the spin axis change, causing a change in predicted orientation of elliptic craters. We developed a numerical forward model of the effect of obliquity on the orientations of elliptic craters using realistic ensembles of simulated Martian impactor orbits and $\sim$3.5 Gyr-long Martian obliquity simulations. We then used a validated version of a global database of Martian crater ellipticities and orientations (Robbins and Hynek, 2012) and the ages of underlying geologic units (Tanaka et al., 2014) to invert for the true Martian obliquity history. From that we construct estimates of the mean obliquity and the number of years with $\epsilon > 40^\circ$ (Fig. 2).

2. Elliptic crater orientations database

The Robbins global Mars crater database (Robbins and Hynek, 2012) contains measurements of crater ellipticities (ratio of major to minor axes lengths) and major axis orientations (absolute azimuth from due North) obtained from fitting ellipses to points traced around crater rims. The publicly available data has a known bug in these parameters where some major axis orientations have been shifted by 90°. While this error has been internally corrected (interested parties can obtain the corrected database from S.J.R.), there has been no independent check of the correction's accuracy. Thus, we carried out an exhaustive search for systematic inter-analyst variability (Appendix A) and found that, restricting our analysis to craters >4 km in diameter and degradation state ≥ 2 (i.e. filtering out the most degraded craters), inter-analyst residuals for both the ellipticity and orientation of craters are not systematically biased. Thus, we concluded that the Robbins database (Robbins and Hynek, 2012) provides a suitable constraint on our model with no systematic inter-analyst error and well quantified random inter-analyst error.

Because our goal is ultimately to compare the population of elliptic crater orientations to predictions made by an ensemble of $\sim$3.5 Gyr Mars obliquity simulations, we must filter out elliptic craters older than $\sim$3.5 Gyr. Individual crater ages are difficult to constrain, but maximum crater ages are constrained by the age of the underlying geologic unit. Thus, we can use the Tanaka et al. (2014) global geologic map of Mars to identify the maximum ages of craters. Because not all of the geologic localities have well determined individual ages due to small surface areas, we rely on the reported geologic epoch of each locality. All terrains listed as Amazonian, early/middle/late Amazonian, Late Hesperian,